

# Field-Driven Hysteresis of the $d=3$ Ising Spin Glass: Hard-Spin Mean-Field Theory

Burcu Yücesoy<sup>1</sup> and A. Nihat Berker<sup>2-4</sup>

<sup>1</sup>*Department of Physics, Istanbul Technical University, Maslak 34450, Istanbul, Turkey,*

<sup>2</sup>*Department of Physics, Koç University, Sarıyer 34450, Istanbul, Turkey,*

<sup>3</sup>*Feza Gürsey Research Institute, TÜBİTAK - Bosphorus University, Çengelköy 34680, Istanbul, Turkey, and*

<sup>4</sup>*Department of Physics, Massachusetts Institute of Technology, Cambridge, Massachusetts 02139, U.S.A.*

Hysteresis loops are obtained in the Ising spin-glass phase in  $d = 3$ , using frustration-conserving hard-spin mean-field theory. The system is driven by a time-dependent random magnetic field  $H_Q$  that is conjugate to the spin-glass order  $Q$ , yielding a field-driven first-order phase transition through the spin-glass phase. The hysteresis loop area  $A$  of the  $Q - H_Q$  curve scales with respect to the sweep rate  $h$  of magnetic field as  $A - A_0 \sim h^b$ . In the spin-glass and random-bond ferromagnetic phases, the sweep-rate scaling exponent  $b$  changes with temperature  $T$ , but appears not to change with antiferromagnetic bond concentration  $p$ . By contrast, in the pure ferromagnetic phase,  $b$  does not depend on  $T$  and has a sharply different value than in the two other phases.

PACS numbers: 75.10.Nr, 75.60.Ej, 64.60.Ht, 05.70.Ln

Frustration and non-equilibrium effects induce complicated ordering behaviors that challenge the methods of statistical physics. Perhaps the most ubiquitous non-equilibrium effect, hysteresis is the current topic of intense fundamental and applied studies. The effects of a spatially uniform linearly driven magnetic field on the ferromagnetic phase of the  $n$ -component vector model in  $d = 3$  [1] and of the pure (no quenched randomness) Ising model in  $d = 2, 3, 4$  [2, 3] have been studied. In these works, the scaling exponents of the hysteresis loop area with respect to the sweep rate are obtained. Spatially uniform pulsed, sinusoidally oscillating, and stochastically varying magnetic fields on the ferromagnetic phase of the pure Ising model in  $d = 2, 3$  [4, 5] and spatially uniform square-wave magnetic fields on the ferromagnetic phase of the pure Ising model in  $d = 2$  [8] have been studied. Two current detailed experimental studies of hysteresis are in Refs.[6, 7].

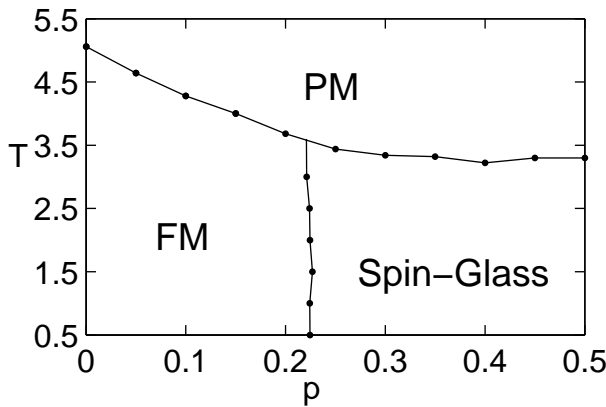


FIG. 1: Phase diagram from hard-spin mean-field theory for the  $d=3$  Ising spin glass. All phase boundaries are second order.

In the present study, hard-spin mean-field theory, developed specifically to respect frustration [9, 10], is used

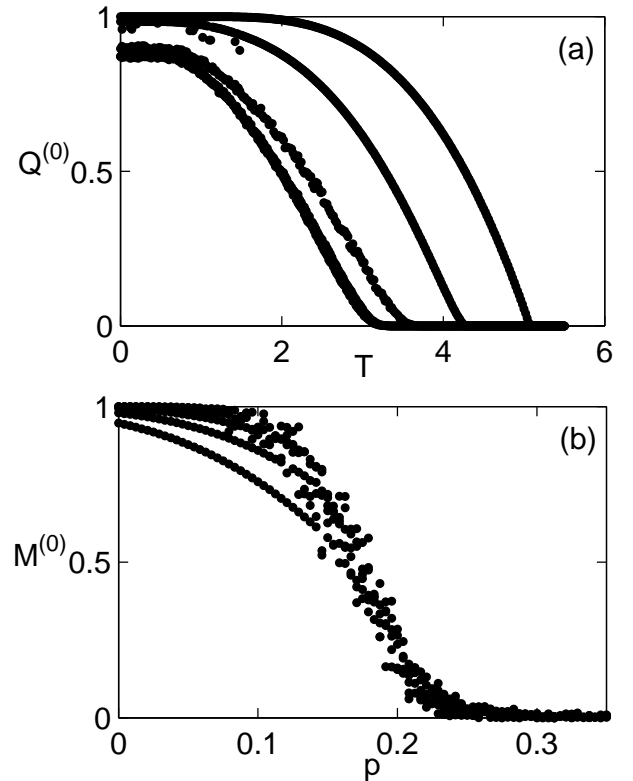


FIG. 2: (a) Equilibrium spin-glass order parameter  $Q^{(0)}$  as a function of temperature  $T = J^{-1}$ . The curves, from top to bottom, are for  $p = 0, 0.1, 0.2, 0.3, 0.5$ . The latter two curves overlap. (b) Equilibrium magnetization  $M^{(0)}$  as a function of concentration  $p$ . The curves, from top to bottom, are for  $T = 0.5, 1.0, 1.5, 2.0, 2.5, 3.0$ .

to study the non-equilibrium behavior of the field-driven first-order phase transition that is implicit, but to-date unstudied, in spin-glass ordering. For the Ising spin-glass on a cubic lattice, the phase diagram is obtained and the temperature- and concentration-dependent ordering of the spin-glass phase is microscopically deter-

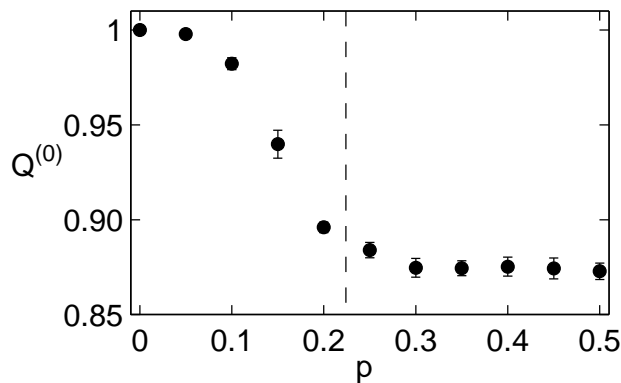


FIG. 3: Zero-temperature spin-glass order parameter  $Q^{(0)}$  as a function of antiferromagnetic bond concentration  $p$ , obtained by averaging over 10 realizations, with the standard deviation being used as the error bar. The dashed line indicates the transition between the two phases, whose position is obtained from the phase diagram in Fig.1.

mined. The random magnetic field that is conjugate to this microscopic order is then identified and used to induce a first-order transition and hysteresis loops. We find qualitatively and quantitatively contrasting scaling behaviors in spin-glass, quenched random-bond ferromagnetic, and pure ferromagnetic phases of the system.

The model is defined by the Hamiltonian

$$-\beta H = \sum_{\langle ij \rangle} J_{ij} s_i s_j + \sum_i H_i(t) s_i, \quad (1)$$

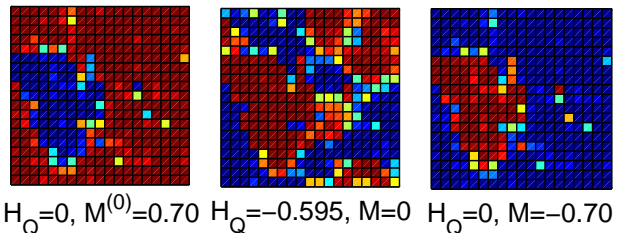
where  $s_i = \pm 1$  at each site  $i$  of a cubic lattice and  $\langle ij \rangle$  denotes summation over nearest-neighbor pairs. The bond strengths  $J_{ij}$  are equal to  $-J$  with quenched probability  $p$  and  $+J$  with probability  $1-p$ , respectively corresponding to antiferromagnetic and ferromagnetic coupling.  $H_i(t)$  is a linearly swept quenched random magnetic field, itself determined, as explained below, by the spin-glass local order of this system.

For our calculations we use the hard-spin mean-field theory [9, 10, 11, 12, 13, 14, 15, 16, 17, 18, 19, 20, 21, 22, 23], a method which is nearly as simply implemented as the conventional mean-field theory but which conserves frustration by incorporating the effect of the full magnitude of each spin. The self-consistent equation for local magnetizations  $m_i$  in hard-spin mean-field theory is

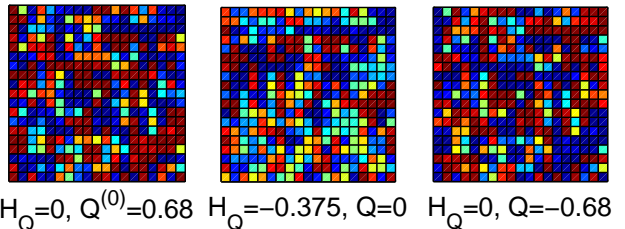
$$m_i = \sum_{\{s_j\}} \left[ \prod_j P(m_j, s_j) \right] \tanh \left( \sum_j J_{ij} s_j + H_i(t) \right), \quad (2)$$

where the sum  $\{s_j\}$  is over all interacting neighbor configurations and the sum and the product over  $j$  are over all sites that are coupled to site  $i$  by interaction  $J_{ij}$ . The single-site probability distribution  $P(m_j, s_j)$  is  $(1 + m_j s_j)/2$ . The hard-spin mean-field theory has

### Local Magnetizations in the Ferromagnetic Hysteresis Loop



### Local Magnetizations in the Spin-Glass Hysteresis Loop



### Local Magnetizations in the Paramagnetic Phase

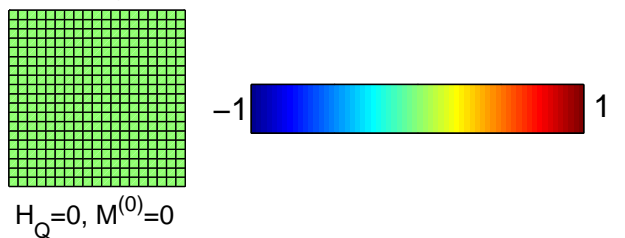


FIG. 4: The top-row figures are from a hysteresis loop in the ferromagnetic phase with quenched random antiferromagnetic bonds,  $T = 1.5, p = 0.15, h = 0.005$ . The middle-row figures are from a hysteresis loop in the spin-glass phase,  $T = 1.5, p = 0.4, h = 0.005$ . Left: calculated equilibrium local magnetizations  $m_i^{(0)}$  in a cross-section of the three-dimensional system. A hysteresis loop is started from these systems. Middle: local magnetizations  $m_i(t)$  at the first cancellation point,  $M(t) = 0$  (top row) and  $Q(t) = 0$  (middle row), of the first hysteresis loop. Left: local magnetizations at the first reversal point,  $M(t) = -M(0)$  and  $Q(t) = -Q(0)$ , which occurs when the first hysteresis half-loop is completed. The bottom cross-section shows the vanishing equilibrium local magnetizations everywhere in the paramagnetic phase, to be contrasted with the spin-glass cross-section immediately above it: the global magnetization  $M^{(0)} = 0$  in both cases.

been used in time-dependent systems, in the study of field-cooled and zero-field cooled magnetizations in spin glasses.[17]

*Equilibrium Phase Diagram* - The equilibrium local magnetizations  $m_i^{(0)}$  are determined by simultaneously solving  $N$  coupled Eqs.(2) for all  $N$  sites  $i$  of the system, at zero external magnetic field,  $H = 0$ . For  $0 < p < 1$ , the system is degenerate, and many local magnetization solutions exist and are reached by hard-spin mean-field

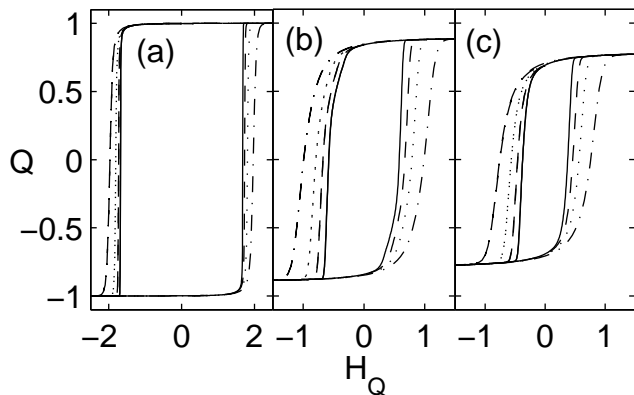


FIG. 5: Hysteresis loops for different values of the sweep rate  $h$  for (a) the pure ferromagnetic phase,  $p = 0$ , (b) the ferromagnetic phase with quenched random antiferromagnetic bonds,  $p = 0.15$ , (c) the spin-glass phase,  $p = 0.4$ , all at  $T = 1.5$ . The loops are, from outer to inner, for sweep rates  $h = 0.05, 0.02, 0.01, 0.005$ .

theory. The phase diagram (Fig.1) is obtained from temperature  $T = J^{-1}$  and concentration  $p$  scans of the equilibrium spin-glass order parameter  $Q^{(0)} = \frac{1}{N} \sum_i m_i^2$  and magnetization  $M^{(0)} = \frac{1}{N} \sum_i m_i$ , illustrated in Fig.2, obtained by averaging over 20 realizations for a  $N = 20^3$  spin system. The results do not change if a larger system is used. In the resulting phase diagram shown in Fig.1, the transition temperatures are gauged by comparing  $T_C$  at  $p = 0$ : The precise value [24] is 4.51, the ordinary mean-field value is 6, the value obtained here is 5.06. Thus, the transition temperatures are exaggerated as expected from a mean-field theory, but considerably improved over ordinary mean-field theory. Our obtained transition concentrations between the ferromagnetic and spin-glass phases are  $p = 0.22$ , in excellent agreement with the precise value of  $p = 0.23$  [25].

Fig.3 shows the zero-temperature spin-glass order parameter  $Q^{(0)}$  as a function of antiferromagnetic bond concentration  $p$ . It seen that, as soon as frustration is introduced via the antiferromagnetic bonds, order does not saturate at zero temperature, both in the ferromagnetic and spin-glass phases, the latter of course showing more unsaturation. Moreover, the left column of Fig.4 shows the equilibrium local magnetizations  $m_i$  in a cross-section of the system, in the ferromagnetic and spin-glass phases. These magnetization cross-sections are remarkably similar to the renormalization-group results [26] and are consistent with the chaotic rescaling picture of the spin-glass phase [27].

*Spin-Glass Hysteresis Loops* - The quenched random magnetic field that is conjugate to the microscopic order is  $H_i(t) = H_Q(t)m_i^{(0)}$  in Eq.(1), where the  $m_i^{(0)}$  are the equilibrium local magnetizations obtained with Eq.(2) for a given  $T, p$ . Hysteresis loops in the spin-glass order  $Q(t) = \frac{1}{N} \sum_i m_i(t)m_i^{(0)}$  are obtained in the ordered

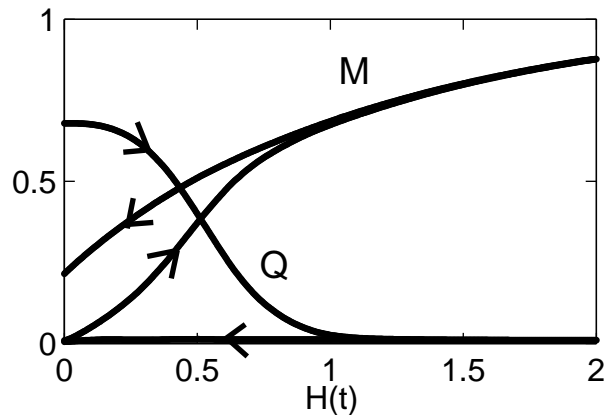


FIG. 6: Spin-glass order parameter  $Q(t)$  and uniform magnetization  $M(t)$  curves obtained when, in the spin-glass phase, the uniform magnetic field  $H(t)$  is turned on and then off with sweep rate  $h = 0.005$ . In this figure,  $p = 0.4, T = 1.5$ .

phases, spin-glass or ferromagnetic, by cycling  $H_Q(t)$  at constant  $T, p$ , via a step of magnitude  $h$  for each time unit. Thus, at time  $t = 0$ ,  $Q(t = 0) = Q^{(0)}$ , the equilibrium spin-glass order parameter. A time unit is  $N$  updatings of Eq.(2) at randomly selected sites. Thus,  $h$  is the sweep rate of the linearly driven [1, 2, 3] magnetic field. For comparison, it takes of the order of  $40N$  random updatings to establish equilibrium in the pure ferromagnetic phase and  $2000N$  random updatings to establish equilibrium in the spin-glass phase. Thus, during the sweeps, each time step with  $N$  updatings systematically moves in the direction of the changed external field but, within the loops, does not catch up with equilibrium. The resulting hysteresis curves are illustrated in Figs.5. After one cycling, the subsequent hysteresis loops for a given sweep rate coincide, and are shown in Figs.5 and used in the scaling analysis further below.

*Cycling Effect of a Uniform Magnetic Field on Spin-Glass Order* - As a contrast to the hysteretic effect of the conjugate quenched random magnetic field  $H_Q(t)$  introduced above, Fig.6 shows the effect on the spin-glass phase of turning on and then off a uniform magnetic field  $H(t)$  at a sweep rate  $h$ . As expected, the spin-glass order  $Q(t)$  starts at a finite value and returns to zero, while the uniform magnetization  $M(t) = \frac{1}{N} \sum_i m_i(t)$  starts at zero and returns to a finite value.

*Spin-Glass Hysteresis Area Scaling* - The energy dissipation of a first-order phase transition is obtained from the hysteresis area  $A$  of the  $Q - H_Q$  curve:  $A = \oint Q dH_Q$ . At fixed  $T, p$ , the loop area  $A$  decreases with decreasing sweep rate  $h$  and finally reaches a value of  $A_0$ . The area can be scaled as  $A = A_0 + f(T)h^b$ . [3] The  $(A - A_0)$  versus sweep rate  $h$  scaling curves are shown in Figs.7, for the pure ferromagnetic, quenched random-bond ferromagnetic, and spin-glass phases for various temperatures, where  $A_0$  is fitted. The resulting sweep-rate exponents

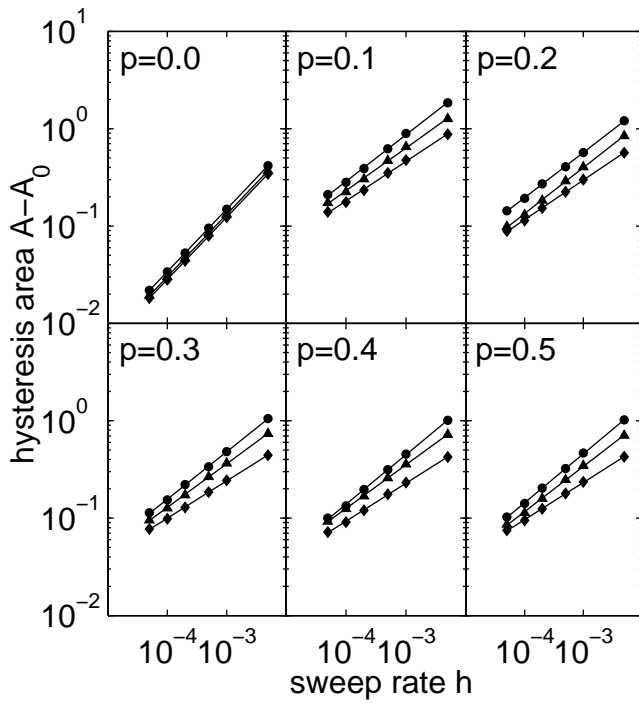


FIG. 7: The hysteresis area  $A - A_0$  versus sweep rate  $h$  scaling curves for  $T = 1.0$  (●),  $1.5$  (▲),  $2.0$  (◆) at different concentrations  $p$ .

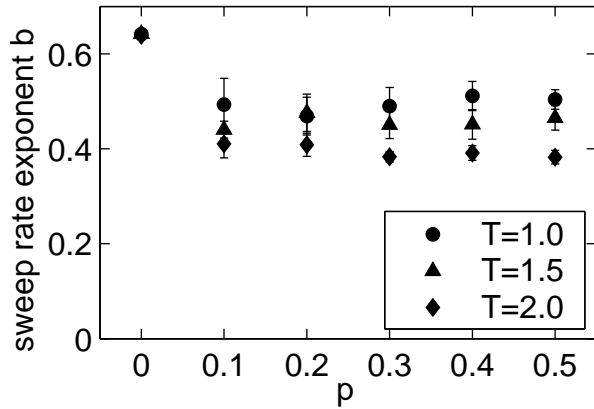


FIG. 8: The sweep-rate scaling exponent  $b$  versus concentration  $p$  for  $T = 1.0, 1.5, 2.0$ . These results are obtained by averaging over 10 realizations, with the standard deviation being used as the error bar.

$b$  are given in Fig.8 and Table I. From these results, we deduce that in the pure ferromagnetic phase,  $p = 0$ , the exponent  $b$  is independent of temperature, as found previously [3]. However, the value of  $b = 0.64$  that we find here, under hard-spin mean-field dynamics, is distinctly different from that of  $b = 2/3$  found in Ref.[3] under ordinary mean-field dynamics, thereby constituting a different dynamic universality class. By contrast, in the quenched random-bond ferromagnetic phase and in the

$T$	$p = 0$	$p = 0.1$	$p = 0.2$	$p = 0.3$	$p = 0.4$	$p = 0.5$
1.0	0.64	$0.49 \pm 0.06$	$0.47 \pm 0.04$	$0.49 \pm 0.04$	$0.51 \pm 0.03$	$0.50 \pm 0.02$
1.5	0.64	$0.44 \pm 0.02$	$0.48 \pm 0.04$	$0.45 \pm 0.03$	$0.45 \pm 0.03$	$0.47 \pm 0.03$
2.0	0.64	$0.41 \pm 0.03$	$0.41 \pm 0.02$	$0.38 \pm 0.01$	$0.39 \pm 0.02$	$0.38 \pm 0.01$

TABLE I: The sweep-rate scaling exponents  $b$  at different temperatures and concentrations in the ferromagnetic and spin-glass phases.

spin-glass phase, the value of  $b$  is distinctly smaller than that in the pure ferromagnetic phase, and dependent on temperature. Across both of these two phases, there appears to be no dependence of  $b$  on concentration.

We thank Y. Öner for drawing our attention to hysteresis problems in frustrated systems and for useful discussions. We thank M. Hinczewski, A. Kabakçioğlu, and M.C. Yalabık for useful discussions. This research was supported by the Scientific and Technical Research Council (TÜBİTAK) and by the Academy of Sciences of Turkey.

- [1] F. Zhong, J.X. Zhang, and G.G. Siu, J. Phys.: Cond. Matt. **6**, 7785 (1994).
- [2] F. Zhong, J.X. Zhang, and L. Xiao, Phys. Rev. E **52**, 1399 (1995).
- [3] G.P. Zheng and J.X. Zhang, J. Phys.: Cond. Matt. **10**, 1863 (1998).
- [4] B.K. Chakrabarti and M. Acharyya, Rev. Mod. Phys. **71**, 847 (1999).
- [5] A. Chatterjee and B.K. Chakrabarti, Phase Tr. **77**, 581 (2004).
- [6] M.S. Pierce, C.R. Buechler, L.B. Sorensen, S.D. Kevan, E.A. Jagla, J.M. Deutsch, T. Mai, O. Narayan, J.E. Davies, K. Liu, G.T. Zimanyi, H.G. Katzgraber, O. Hellwig, E.E. Fullerton, P. Fischer, and J.B. Kortright, Phys. Rev. B **75**, 144406 (2007).
- [7] E. Bonnot, R. Romero, X. Illa, L. Manosa, A. Planes, and E. Vives, Phys. Rev. B **76**, 064105 (2007).
- [8] D.T. Robb, P.A. Rikvold, A. Berger, and M.A. Novotny, Phys. Rev. E **76**, 021124 (2007).
- [9] R.R. Netz and A.N. Berker, Phys. Rev. Lett. **66**, 377 (1991).
- [10] R.R. Netz and A.N. Berker, J. Appl. Phys. **70**, 6074 (1991).
- [11] J.R. Banavar, M. Cieplak, and A. Maritan, Phys. Rev. Lett. **67**, 1807 (1991).
- [12] R.R. Netz and A.N. Berker, Phys. Rev. Lett. **67**, 1808 (1991).
- [13] R.R. Netz, Phys. Rev. B **46**, 1209 (1992).
- [14] R.R. Netz, Phys. Rev. B **48**, 16113 (1993).
- [15] A.N. Berker, A. Kabakçioğlu, R.R. Netz, and M.C. Yalabık, Turk. J. Phys. **18**, 354 (1994).
- [16] A. Kabakçioğlu, A.N. Berker, and M.C. Yalabık, Phys. Rev. E **49**, 2680 (1994).
- [17] E.A. Ames and S.R. McKay, J. Appl. Phys. **76**, 6197 (1994).
- [18] G.B. Akgüç and M.C. Yalabık, Phys. Rev. E **51**, 2636 (1995).
- [19] J.E. Tesiero and S.R. McKay, J. Appl. Phys. **79**, 6146,

- (1996).
- [20] J.L. Monroe, Phys. Lett. A **230**, 111 (1997).
- [21] A. Pelizzola and M. Pretti, Phys. Rev. B **60**, 10134 (1999).
- [22] A. Kabakçioğlu, Phys. Rev. E **61**, 3366 (2000).
- [23] H. Kaya and A.N. Berker, Phys. Rev. E **62**, R1469 (2000).
- [24] A.M. Ferrenberg and D.P. Landau, Phys. Rev. B **44**, 5081 (1991).
- [25] Y. Ozeki and N. Ito, J. Phys. A **31**, 5451 (1998).
- [26] D. Yeşiltepe and A.N. Berker, Phys. Rev. Lett. **78**, 1564 (1997).
- [27] S.R. McKay, A.N. Berker, and S. Kirkpatrick, Phys. Rev. Lett. **48**, 767 (1982).